metals

MDPI

Article

Stress Corrosion Cracking Behaviour of Dissimilar Welding of AISI 310S Austenitic Stainless Steel to 2304 Duplex Stainless Steel

Thiago AmaroVicente [1], Leonardo Albergaria Oliveira [1], Edmilson Otoni Correa [1,*], Reginaldo Pinto Barbosa [2], Vanessa Bawden P. Macanhan [1] and Nelson Guedes de Alcântara [3]

[1] Instituto de Engenharia Mecânica, Universidade Federal de Itajuba, Av. BPS, 1303, Pinheirinho, Itajubá 37500-903, Minas Gerais, Brazil; thiagofis@hotmail.com (T.A.V.); leonardoeng1@gmail.com (L.A.O.); vbawden@lna.br (V.B.P.M.)

[2] Aperam South America, Praça 1º de maio, S/N, Centro, Timóteo 35180-000, Minas Gerais, Brazil; reginaldo.barbosa@aperam.com

[3] Departamento de Materiais (DEMA), Universidade Federal de São Carlos, Av. Washington Luis, Km 435, São Carlos 13565-905, São Paulo, Brazil; nelsong@ufscar.br

* Correspondence: ecotoni@unifei.edu.br; Tel.: +55-35-3629-1028

Received: 7 December 2017; Accepted: 5 February 2018; Published: 20 March 2018

Abstract: The influence of the weld metal chemistry on the stress corrosion cracking (SCC) susceptibility of dissimilar weldments between 310S austenitic stainless steel and 2304 duplex steels was investigated by constant load tests and microstructural examination. Two filler metals (E309L and E2209) were used to produce fusion zones of different chemical compositions. The SCC results showed that the heat affected zone (HAZ) on the 2304 base metal side of the weldments was the most susceptible region to SCC for both filler metals tested. The SCC results also showed that the weldments with 2209 duplex steel filler metal presented the best SCC resistance when compared to the weldments with E309L filler metal. The lower SCC resistance of the dissimilar joint with 309L austenitic steel filler metal may be attributed to (1) the presence of brittle chi/sigma phase in the HAZ on the 2304 base metal, which produced SC cracks in this region and (2) the presence of a semi-continuous delta-ferrite network in the fusion zone which favored the nucleation and propagation of SC cracks from the fusion zone to HAZ of the 2304 stainless steel. Thus, the SC cracks from the fusion zone associated with the SC cracks of 2304 HAZ decreased considerably the time-of-fracture on this region, where the fracture occurred. Although the dissimilar weldment with E2209 filler metal also presented SC cracks in the HAZ on the 2304 side, it did not present the delta ferrite network in the fusion zone due to its chemical composition. Fractography analyses showed that the mixed fracture mode was predominant for both filler metals used.

Keywords: dissimilar weldments; stress corrosion cracking; stainless steels

1. Introduction

Austenitic stainless steel 310S is widely used for high-temperature applications in the petrochemical, nuclear, geothermal, and oil and gas industries due to its high resistance to oxidation, hydrogen embrittlement and corrosion [1–3].

In many of these industrial applications, fusion welding is the main method used to join or repair the components and it may contribute to the particular case of corrosion denominated Corrosion Stress Cracking (SCC). SCC is the main corrosion failure mode for 310S stainless steels and it is characterized by the slow nucleation and propagation of cracks on the material under the synergic interaction of mechanical tension and a specific corrosive environment [3,4]. In general, the nucleation of stress

corrosion cracks occurs at stress levels below the yield stress of the materialand SCC full failure could occur at stresses below the material's ultimate tensile strength [4–7].

Because of the lower SCC resistance of 310S stainless steel, Ni-based superalloys and duplex stainless steels (DSS) are attractive materials and technical and economical candidates to replace 310S in several high temperature applications where SCC resistance is a requirement. DSS, which possess good strength, high toughness and excellent resistance to SCC and localized corrosion (pitting) are more recommended in applications where the maximum working temperatures are approximately 350 °C. As a result, the necessity of joining DSS and austenitic 310S stainless steel is indispensable [3,8].

According to literature [6,9,10], during dissimilar welding involving particularly duplex and austenitic stainless steels, certain problems can arise during the joining of several components. In duplex steels, during welding, the heat affected zone (HAZ) often experiences critical temperatures that are sufficient to produce almost fully ferrite in this region. As cooling starts, the formed ferrite undergoes a solid-state transformation to austenite from the grain boundary and then continues in the ferrite grains. The extent of ferrite to austenite transformation depends on the base metal and filler metal composition and welding parameters. Considering that in the welding process, the cooling rate is high, significant ferrite content can remain in the HAZ and precipitation of brittle secondary phases such as sigma (σ), chi (χ) and chromium nitride can occur at locations that have reached temperatures above 800 °C with suppression of ferrite-to austenite phase transformation. This can significantly reduce mechanical properties, pitting and stress corrosion cracking resistance of the stainless steel dissimilar weldment [9,10].

It is worthwhile mentioning that sigma and chi phases are formed mainly of iron and chromium, but they may contain small amounts of molybdenum as well. As a result, variations in the chromium and molybdenum contents in the filler metal and base metal chemistry modify the kinetic reactions and modify significantly the elemental partitioning and, consequently, the volume fraction of delta ferrite and sigma phase. According to literature [9,10], when the base metal and/or filler metal contain levels of chromium above 20% and molybdenum is in small amount, sigma and chi phases precipitation is very prone to occur in the HAZ of the dissimilar stainless steel weldment involving duplex steels.

Concerning dissimilar welding involving austenitic stainless steels and other type of stainless steel with quite different contents of Cr, Ni and Mo, prior works [11,12] have reported that the delta ferrite content present in the weld metal has a significant influence on the susceptibility to stress corrosion cracking of the weldment once this phase is electrochemically more active than the austenite phase, resulting in preferential corrosion attack of the weld regions enriched to these phases, when exposed to an aggressive environment.

In an attempt to mitigate the problems mentioned above and improve the stress corrosion cracking resistance of these dissimilar weldments, one of the most important issues is the evaluation of proper filler metal for welds between DSS and austenitic stainless steels. Basically, these evaluations consist of investigating filler metal composition on the delta ferrite content and on elemental partitioning in weld metal and HAZ in order to reduce the susceptibility to stress corrosion cracking and the influence of the welding thermal cycle (which is directly dependent on the welding parameters).

Therefore, this study aims to evaluate the influence of two different filler metals (E309L and E2209) on the microstructure and on the SCC resistance of dissimilar stainless steel weldments between 310S austenitic stainless steel and 2304 duplex stainless steel in an environment containing boiling chloride. The correct selection of the filler metal may be an efficient practice to minimize the occurrence of SCC in repair welds of industrial equipment.

2. Experimental Procedure

2.1. Welding

In this study, 310S austenitic stainless steel and 2304 duplex stainless sheets of 3 mm thickness were used as base materials; 1.2 mm diameter wires of E309L and E2209 stainless steels were used as addition metals. Table 1 presents the chemical compositions of the base and filler metals used.

Table 1. Chemical composition (% weight) of the base and filler metals.

Materials	C	Mn	Si	Cr	Ni	Mo	N
310S	0.08	2.00	1.50	25.00	20.50	-	-
2304	0.02	1.36	0.39	22.23	3.61	0.31	0.11
E2209	0.03	1.47	0.57	22.50	9.20	3.12	0.14
E309L	0.03	0.69	0.96	24.00	13.00	0.75	-

It can be noted from Table 1 that the most dominant difference in composition of the metals is the presence of a higher amount of Cr and Ni in the E309L filler metal and a higher amount of Mo in the E2209 filler metal.

The automatic welding was carried out with a single deposition on flat position on 70 mm × 255 mm × 3 mm plates, using the conventional Gas Metal Arc Welding (GMAW) process. The welding parameters used in this work are shown in Table 2.

Table 2. Welding conditions used in this study.

Gas Flow (L/min)	Shielding Gas (%)	Voltage (V)	Current (A)	Travel Speed (m/min)	Wire Feed Speed (m/min)
14	Argon-2% O_2	19	122	0.35	4

2.2. Stress Corrosion Cracking (SCC) Testing

To evaluate the SCC behaviour of the weldments in aerated boiling 43% $MgCl_2$ test solution at 140 ± 2 °C, a constant-load device was used. 3 mm thick smooth rectangular tensile specimens (Figure 1) were used in the SCC tests. The geometry and finishing procedures of the specimens were in accordance with ASTM G58 [13] and ASTM E8 [14] standards.

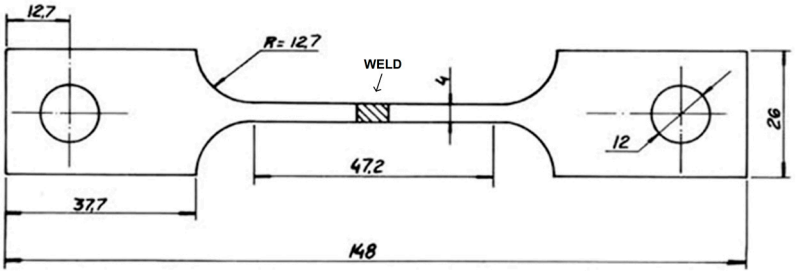

Figure 1. Design of the smooth tensile specimen used in stress corrosion cracking (SCC) tests (unit: mm).

Specimens and test solution were confined in a glass recipient which was coupled to a reflow condenser so that all measurements were continuously monitored under closed-circuit conditions. Tests were carried out at constant of 230 MPa, which was related with SCC failure in $MgCl_2$ for austenitic stainless steels weld metals [15]. Six SCC tests were carried out for each weld metal studied. Time-to-failure was the parameter used to evaluate the SCC resistance of the weldments.

2.3. Microstructural Characterization

After SCC tests, specimens were cut, grinded with abrasive paper 1000 grit, polished up to 1 µm surface finish and etched electrolytically in 10% oxalic acid to examine the microstructure of the weldments. In general, for this etch, ferrite appears as a dark gray phase and austenite appears as a bright gray phase. Microstructural examinations of the specimens were carried out using standard optical microscopy coupled to an image analysis system, scanning electron microscopy (SEM, model Evo MA 15, ZEISS, Oberkochen, Germany) and X-ray Diffraction (XRD, model X'Pert PRO, PANalytical, Eindhoven, The Netherlands).

3. Results and Discussion

SCC Results and Microstructure

As mentioned before, the "time-to-fracture" of the specimens was the parameter adopted to evaluate the susceptibility to the stress corrosion cracking of the weldments. Table 3 shows the average time and temperature values of the test for both filler metals.

Table 3. SCC tests' results.

Weld Metal	Temperature (°C)	Time-to-Fracture (min)
ER 2209	140± 2	213 ± 5
E309L	140 ± 2	73 ± 4

From Table 3, it can be observed that the time-to-fracture of the specimens using filler metal E2209 was approximately 3 times superior to the time-to-fracture observed for E309L filler metal, strongly indicating that welds carried out using filler metal E2209 were significantly more resistant to SCC than those carried out using the filler metal E309L.

Figures 2 and 3 show the microstructures of dissimilar weldments between 310S and 2304 stainless steels after SCC tests. For both weld metals studied, the rupture of the specimens always occurred in the HAZ on the 2304 duplex metal base side, that is, the HAZ of 2304 duplex steel was the most susceptible region to stress corrosion cracking.

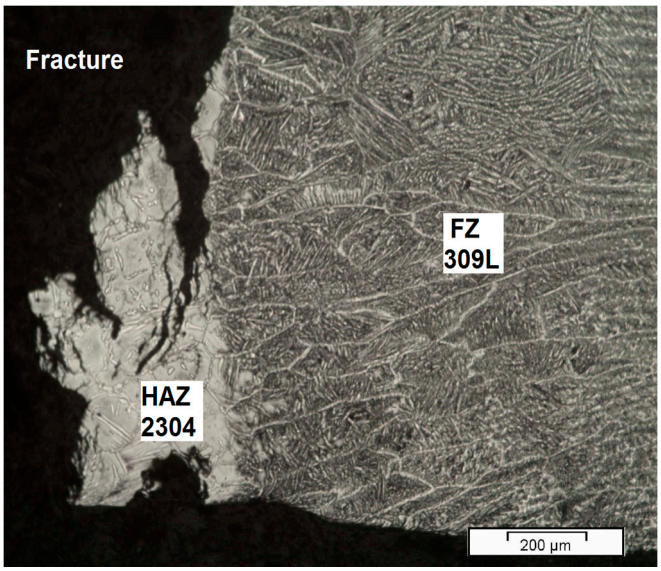

Figure 2. Microstructure of dissimilar weldment with 309L weld metal showing stress corrosion cracks in the heat affected zone (HAZ) on the 2304 duplex stainless steels (DSS) side.

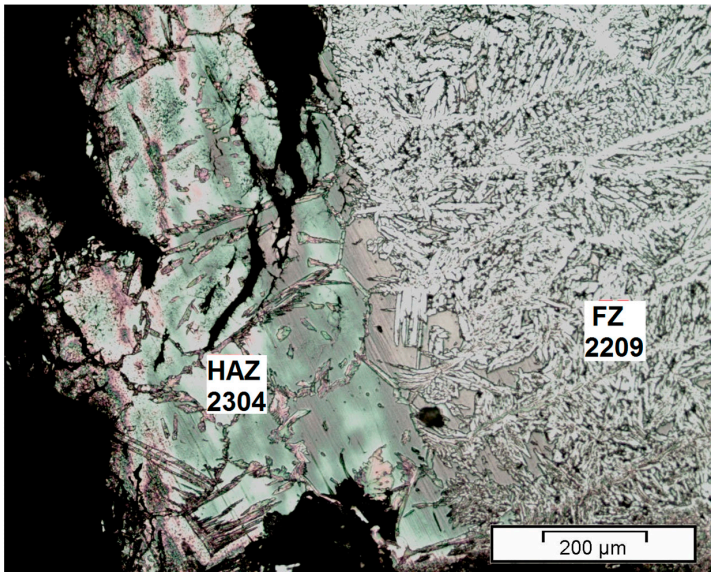

Figure 3. Microstructure of dissimilar weldment with 2209 weld metal showing stress corrosion cracks in the HAZ on the 2304 DSS side.

The higher susceptibility to SCC in HAZ on the 2304 steel side than in HAZ on the 310S steel side, for both filler metals, may be attributed mainly to two reasons: (1) the presence of higher content of ferrite in this zone as indicated by higher intensity of the ferrite peak in comparison with the austenite peak in the XRD analysis shown in Figure 4. It is worthwhile mentioning that in duplex steels, the intensities of austenite and ferrite peaks is approximately the same once the proportion of these phases in duplex steels is 50:50. According to Labanowski [16], the increase of ferrite amount in HAZ is associated to the higher Cr and lower Ni contents in the base metal of 2304 duplex steel and the slower cooling rate of this zone due to the welding heat input. (2) the precipitation of sigma (σ) and/or chi (χ) phases in the HAZ of 2304 duplex steel as shown in microstructural and XRD analysis (see Figures 4 and 5). EDS Microanalyses in the black precipitates shown in Figure 5 indicated that they are widely enriched of Fe (75.3%) and Cr (24.3%) and presented a small amount of Mo (0.4%), which are the main forming elements of sigma and/or chi phases. According to Silva et al. [9], during the welding, these phases are formed in the HAZ at locations that have reached temperatures above 800 °C by eutectoid transformation of part of ferrite present in HAZ. These phases reduce considerably the toughness and the resistance to SCC.

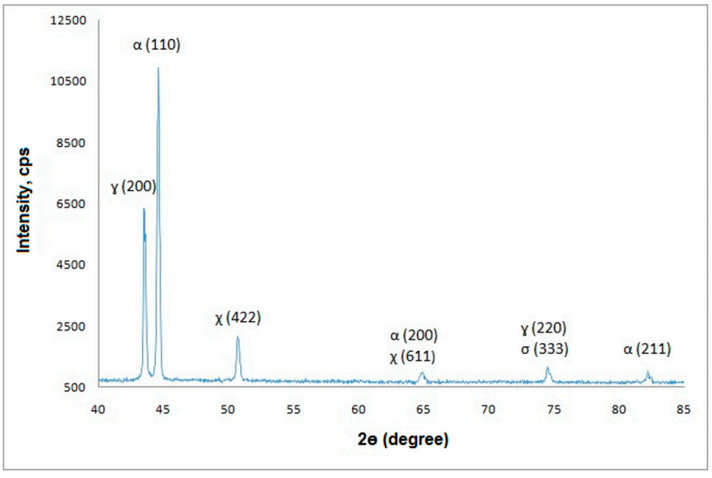

Figure 4. X-ray diffraction pattern of 2304 DSS HAZ.

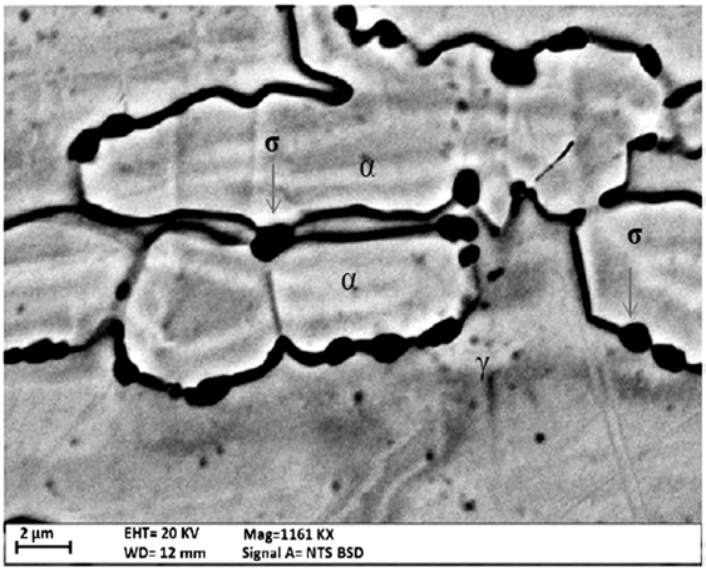

Figure 5. Microstructure of the HAZ of dissimilar weldment with 309L weld metal showing precipitates in the austenite/ferrite interface (chi and/or/sigma phase).

In order to clarify the SCC mechanism, detailed microscopic examinations of cross section taken from fracture areas showed that cracks propagate along the coarse structure of HAZ (Figure 6). Cracks were initiated at the austenite-ferrite phases' boundaries, e propagated along phase boundaries and/or ferrite grains.

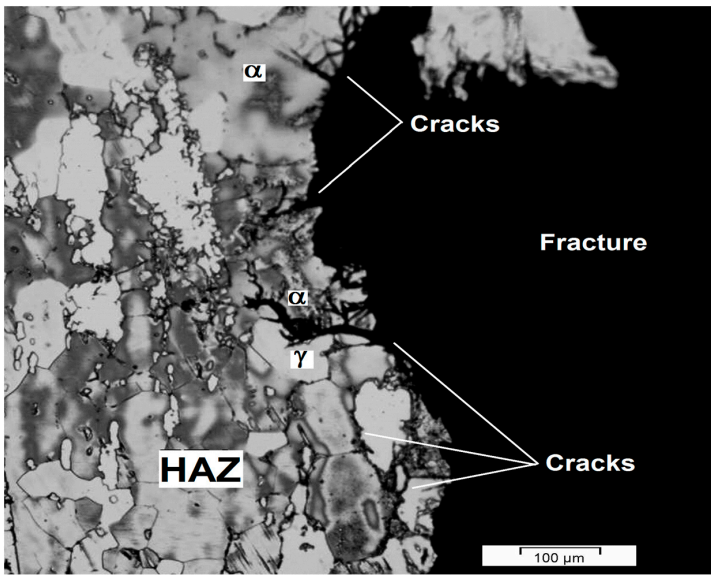

Figure 6. Transverse section of the fracture area in 2304 HAZ. Note cracks in the austenite/ferrite interface and in the ferrite phase.

Furthermore, Figure 7 shows the fracture surface from HAZ of 2304 duplex steel. As can be seen, a mixed fracture mode was observed. It is characterized by the presence of multi-faceted grains with a fibrous appearance and islands of dimples. This fracture surface confirms the lower toughness of this region due to the presence of brittle secondary phases and ferrite in this region.

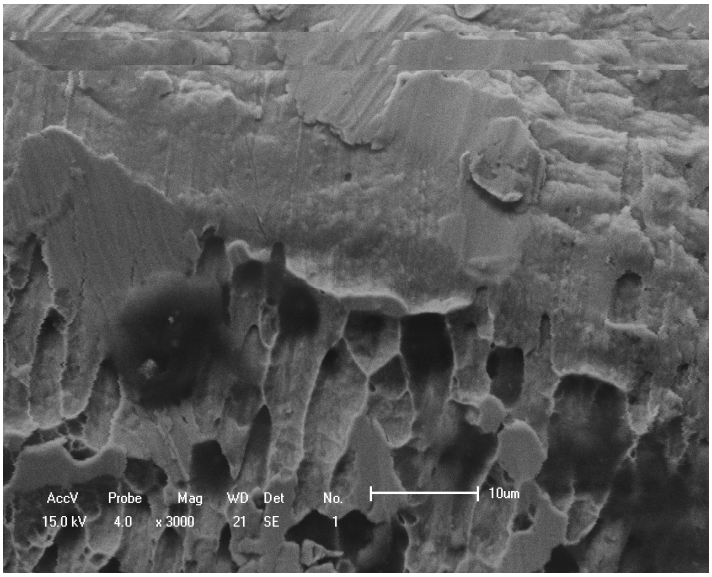

Figure 7. Fracture surface of the HAZ of 2304 DSS showing a mixed fracture mode. Note the presence of grain facets with fibrous appearance and islands of dimples.

Finally, it is important to investigate the reason for which the weldments using E309L filler metal presented significantly lower SCC resistance (smaller fracture time) considering that in these weldments, the most susceptible region was also the HAZ on the 2304 base metal side.

Microstructural examinations strongly indicated that, besides the presence of sigma phase and higher content of ferrite in HAZ of 2304 duplex steel, the presence in the 309L weld metal of a semi-continuous delta-ferrite network distributed in the austenite matrix contributed significantly to the lower SCC resistance of weldment using E309L filler metal (Figures 8 and 9). According to literature [17], the SCC propagation occurs under a relatively straight path along the ferrite boundaries (more electrochemically active) which is attacked more easily by the environment than the austenitic phase.

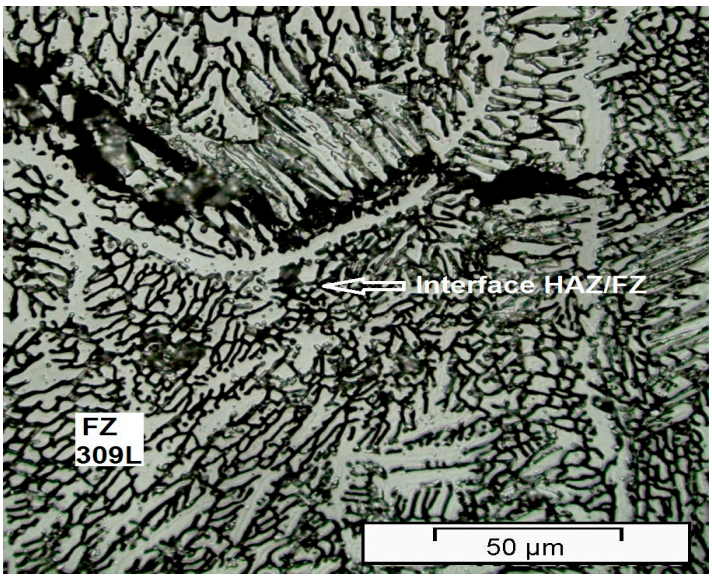

Figure 8. Microstructure showing the presence of a semi-continuous delta ferrite network in the fusion zone of the dissimilar weldment with 309L weld metal.

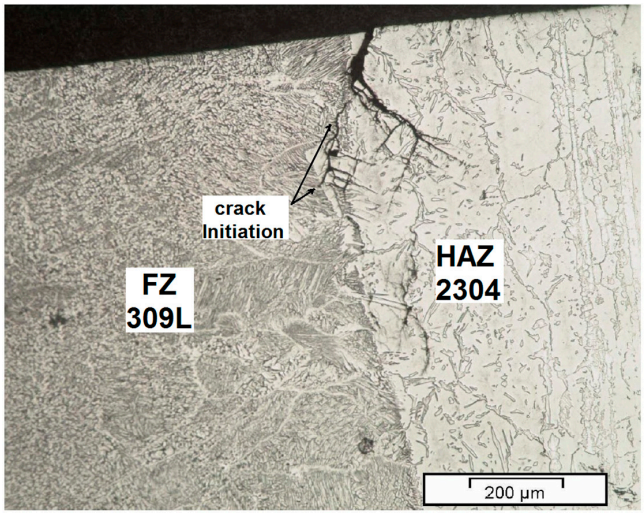

Figure 9. Microstructure showing the presence of cracks in fusion zone of 309L weld metal and in HAZ of the 2304 DSS.

Thus, the cracks initiated in the austenitic weld metal (more susceptible to SCC) near the interface zone propagated towards the HAZ of 2304 duplex steel and associated with the cracks already present in this zone, accelerating the fracture of the specimen and reducing the time-to fracture (Figure 9). According to Nishimura et al. [15], SC cracks propagating from the weld metal to the HAZ interface region could cease when reaching the interface region. However, with the presence of brittle secondary phases in HAZ, the crack propagation can continue alongside this zone.

In order to understand better why the dissimilar weldment from 310S steel side was more resistant to SCC, Figure 10 shows the microstructure of 310S HAZ adjacent to 309L weld metal (more susceptible to SCC). Some little small cracks can be observed in the 310S HAZ and a larger crack can be observed in the 309L fusion zone. From the figure, the presence of large austenite grains with cold deformation twins in some of them can be observed, as well as the absence of high contents of delta ferrite in the HAZ, which is attributed to the higher nickel content in the 310S steel in comparison with other austenitic stainless steels (see Table 1). Nickel stabilizes the austenite and reduces considerably the formation of delta ferrite in the HAZ during weld cooling.

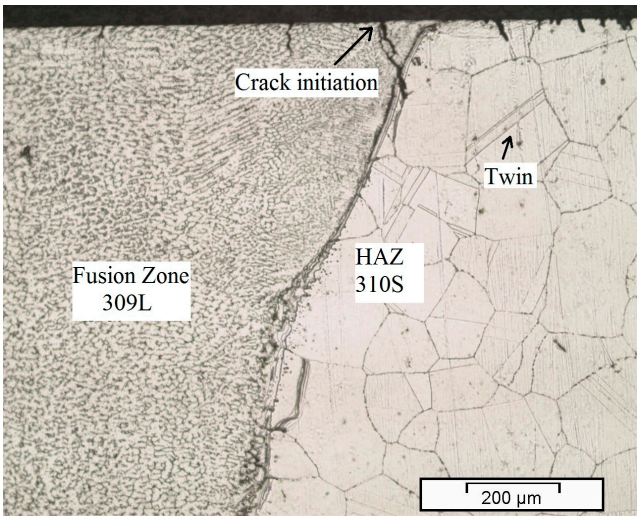

Figure 10. Microstructure showing the presence of austenite and small cracks in the HAZ of the 310S stainless steel. Note also cracks in the 309L weld metal.

Thus, considering that the austenite acts as a cathode, it is more difficultly attacked by the environment, and the lack of presence of high content of delta ferrite (more easily attached) in 310S HAZ, it is possible to affirm that these are the main reasons for the superior SCC resistance of the weldment on the 310S side in relation to the 2304 side for both weld metals.

It is worthwhile mentioning that the microstructure of Figure 10 also strongly indicates that the nucleation and propagation of stress corrosion cracks from the 309L weld metal to HAZ of the base metals really occurs.

4. Conclusions

The following conclusions can be drawn from this study:

1. The higher susceptibility to SCC in HAZ on the 2304 steel side compared to that in HAZ on the 310S steel side, for both filler metals, may be attributed to the presence of a high content of ferrite and the presence of brittle secondary phases which decreased the toughness and SCC resistance of this region.
2. The dissimilar weldment using E309L stainless steel filler metal presented much lower resistance to SCC than the dissimilar joint using 2209 duplex stainless steel. This may be attributed to the simultaneous presence of a semi-continuous delta ferrite (network morphology) in the 309L weld metal which facilitated the nucleation and propagation of cracks from the weld metal to HAZ of 2304. These cracks associated with cracks already present in HAZ of 2304 stainless steel decreased considerably the time of fracture of the weldments.
3. The higher SCC resistance of the 310S HAZ in comparison with the 2304 HAZ may be attributed to the absence of ferrite networks and presence of a great amount of austenite, more resistant to environment attack.
4. In applications where SCC resistance in high temperatures is important, the 2209 filler metal is the best choice for dissimilar welding between 310S austenitic stainless steel and 2304 duplex steel because this filler metal does not present delta ferrite networks in the fusion zone, which makes the nucleation and propagation ofSC cracks difficult from the weld metal to HAZ.

Acknowledgments: The authors are grateful to Aperam South America for supplying the welding consumables and the Brazilian government organizations CNPq, CAPES and FAPEMIG for the financial support.

Author Contributions: E.O.C. conceived and designed the experiments; T.A.V. and L.A.O. performed the experiments; E.O.C. and N.G.A. analyzed the data; R.P.B. contributed reagents/materials/analysis tools; V.B.P.M. wrote the paper

Conflicts of Interest: The authors declare no conflict of interest.

References

1. Lai, C.L.; Tsay, L.W.; Chen, C. Effect of microstructure on hydrogen embrittlement of various stainless steels. *Mater. Sci. Eng. A* **2013**, *584*, 14–20. [CrossRef]
2. Ornek, C.; Idris, S.A.M.; Reccagni, P.; Eingelberg, D.L. Atmospheric induced stress corrosion cracking of grade 2205 duplex stainless steel—Effects of 475 °C embrittlement and process orientation. *Metals* **2016**, *6*, 167. [CrossRef]
3. Kangazian, J.; Shamanian, M.; Ashrafi, A. Dissimilar welding between SAF 2507 stainless steel and Incoloy 825 Ni-based alloy: The role of microstructure on corrosion behavior of weld metals. *J. Manuf. Process.* **2017**, *29*, 376–388. [CrossRef]
4. Ahmad, H.W.; Hwang, J.H.; Lee, J.H.; Bae, D.H. An assessement of the mechanical properties and microstructural analysis of dissimilar material welded joint between alloy 617 and 12 Cr steel. *Metals* **2016**, *6*, 242. [CrossRef]
5. Tavares, S.S.M.; Moura, V.; Costa, V.C.; Ferreira, M.L.R.; Pardal, J.M. Microstructural changes and corrosion resistance of AISI 310S steel exposed to 600–800 °C. *Mater. Charact.* **2009**, *60*, 573–578. [CrossRef]

6. Alyousif, O.; Nishimura, R. On the stress corrosion cracking and Hydrogen embrittlement behavior of austenitic stainless steels in boiling satured magnesium chloride solutions. *Int. J. Corros.* **2012**, *2012*, 462945. [CrossRef]
7. Wu, H.; Li, C.; Fang, K.; Xue, F.; Zhang, G. Effect of machining on the stress corrosion cracking behavior in boiling magnesium chloride solution of austenitic stainless steel. *Mater. Corros.* **2017**, 1–8. [CrossRef]
8. Naffakh, H.; Shamanian, M.; Ashrafizadeh, F. Dissimilar welding of AISI 310 austenitic stainless steel to nickel-based alloy inconel 657. *J. Mater. Process. Technol.* **2009**, *209*, 3628–3639. [CrossRef]
9. Silva, C.C.; Farias, J.P.; Miranda, H.C.; Guimaraes, R.F.; Menezes, J.W.A.; Neto, M.A.M. Microstructural characterization of the HAZ in AISI 444 ferritic stainless steel. *Mater. Charact.* **2008**, *59*, 528–533. [CrossRef]
10. Lippold, J.C.; Kotecki, D.J. *Welding Metallurgy and Weldabilitity of Stainless Steels*, 5th ed.; John Willey & Sons: Hoboken, NJ, USA, 2005.
11. Sui, G.; Charles, E.A.; Congleton, J. The effect of delta-ferrite content on the stress corrosion cracking of austenitic stainless steels in a sulphate solution. *Corros. Sci.* **1996**, *38*, 687–703. [CrossRef]
12. Antunes, P.D.; Correa, E.O.; Barbosa, R.P.; Silva, E.M.; Padilha, A.F.; Guimaraes, P.M. Effect of weld metal chemistry on stress corrosion cracking behavior of AISI 444 ferritic stainless steel weldments in boilingchloride solution. *Mater. Corros.* **2013**, *64*, 415–421. [CrossRef]
13. *Standard Practice for the Preparation of Stress Corrosion Test Specimens for Weldments*; ASTM G58, Annual Book of ASTM Standards; American Society of Testing and Materials: West Conshohocken, PA, USA, 2005.
14. *Standard Methods of Tension Testing of Metallic Materials*; ASTM E8, Annual Book of ASTM Standards; American Society of Testing and Materials: West Conshohocken, PA, USA, 2005.
15. Nishimura, R.; Maeda, Y. SCC evaluation of type 304 and 316 austenitic stainless steels in acidic chloride solutions using the slow strain rate technique. *Corros. Sci.* **2004**, *46*, 769–785. [CrossRef]
16. Labanowski, J. Stress corrosion cracking susceptibility of dissimilar stainless steels welded joints. *J. Achiev. Manuf. Eng.* **2007**, *20*, 255–258.
17. Seifert, H.P.; Ritter, S.; Shoji, T.; Peng, Q.J.; Takeda, Y.; Lu, Z.P. Enviromentally-assisted cracking behavior in the transition region of an alloy 182/SA 508 Cl.2 dissimilar metal welding joint in simulated boiling water reactor normal water chemistry environment. *J. Nucl. Mater.* **2008**, *378*, 197–210. [CrossRef]